Localization of structural zones producing hypersensitive behavior: finite element approach

Morvan Ouisse, Jean-Louis Guyader

Localization of structural zones producing hypersensitive behavior: finite element approach

M. Ouisse J.-L. Guyader

L.V.A. INSA Lyon, 25 bis avenue Jean Capelle, 69621 Villeurbanne Cedex, France

Abstract

On the basis of our previous works (6), one present here a FEM application of a method that allows one to detect structural zones producing hypersensitive behavior. The concept is quite simple, and is cheaper than Monte Carlo simulations. The complete resolution of the problem is done only once, using nominal parameters of the structure, in order to obtain the displacement field. Then, considering another structure, built using variable parameters, chosen in a random way in the acceptable manufacturing range, the finite element assembly procedure is performed. These matrices are finally used to define an indicator in which the displacement field of the nominal solution permits to detect structural zones responsible for hypersensitive behavior. It is based on the computation of energy of a residual displacement field. After a presentation of the basis of this tool, numerical results are presented on a finite element model of a hypersensitive plates network, in which sensitivity problems are linked to angular coupling, and on a cross member beam, which is made up of three spot-welded layers.

Key words: finite elements, localization, vibration, hypersensitivity, error

Email addresses: ouisse@lva.insa-lyon.fr (M. Ouisse), guyader@lva.insa-lyon.fr (J.-L. Guyader).

URL: http://lva.insa-lyon.fr (J.-L. Guyader).

1 Introduction

Serial manufacturing of objects is the reason why studies of uncertainties are becoming more and more important. Classical approaches for uncertainties considerations have a common aim: according to known structural uncertainties (geometry, materials...), one try to estimate variations of responses. Experimental works shown that it was not an easy task (10), (12). In the field of finite element, the most popular approach for uncertainties is the stochastic finite element method (3), (8). The main purpose of sensitivity analysis is to be able to reduce dispersions without increasing manufacturing cost, which is closely related to ranges on which structural parameters can vary.

As far as uncertainties inducing small differences on responses of structures are concerned, this is acceptable. But when hypersensitivity appears, the designed structure can be responsible for some problems: if a very small variation of a given parameter is inducing large differences on responses, two structures which are supposed to be nominally identical can have very different behaviors, in particular when shifting structural eigenfrequencies coincide with cavity ones. This is the reason why a tool that could help one to obtain a low calculation cost information about structural zones which are responsible for hypersensitive behavior could help people during design or analysis stage.

The method proposed here is based on techniques used in finite element model updating (1). The purpose of it is to find zones of FE model that are not in accordance with measured data, which is relatively close to what we need. Using these techniques for other purpose that FE updating has already been done, in particular for damage detection (2), (9). The basic idea is to compare two structures which are supposed to be similar except in a few zones and to detect these zones.

The method has been presented in (6), its principle is quite simple and can be described in two steps:

The first step is to consider the reference structure (named Ω_0), which is the one with nominal parameters. As far as finite element analysis is concerned, assembly of this model is performed to obtain mass and stiffness matrices M_0 and K_0. Then, the eigenvalue problem is solved to obtain eigenvalues ω_0^i and eigenvectors U_0^i.

The second step is to consider a slightly different structure Ω_1, in which structural parameters belong to manufacturing ranges. Then, assembly of this model is performed to obtain mass and stiffness matrices M_1 and K_1, while eigen problem is not solved. A local indicator, which is based on M_1, K_1, ω_0^i and U_0^i is evaluated on elements of the structure in order to find on which zones the solution of reference problem does not match to structure Ω_1.

In this paper use of this method with finite element analysis is detailed. It is limited to modal analysis: the aim is to detect structural zones which are responsible for large dispersions on eigen characteristics.

2 Indicator choice

The main point in the proposed approach is the indicator definition. The one which has been chosen here is commonly used in the field of finite element updating (13), (11). Practically, finite element analyses and formulations have been done using SDT (14), which is a FE toolbox for Matlab. This choice has been made because it is an open FE code, in which programming and modifying algorithms in Matlab language is very easy.

2.1 Expression of used indicator

Two nominally identical structures are considered, which are named Ω_0 and Ω_1. Ω_0 is the reference structure (the one used for complete resolution), while Ω_1 is a slightly different structure from Ω_0. One supposes that assemblies of mass matrices (M_0 and M_1) and stiffness matrices (K_0 and K_1) have been done, and that finite element models of both structures are compatible: degrees of freedom are identical, stored in the same way in matrices and correspond to similar elements. Moreover, stiffness and mass matrices are supposed to be symmetric, definite and positive. Even if these hypotheses are not always necessary to apply the proposed method, they lead to an easier formulation, which is presented here.

The first step is the resolution of the nominal problem, allowing one to obtain n eigenvectors U_0^i and n eigen frequencies ω_0^i, $i = 1 \,\text{to}\, n$. These modes are supposed to be mass normalized. The residual that allows one to localize structural zones in which eigen solution of mode i from reference structure does not verify equations corresponding to modified structure has the following expression:

$$R^i = K_1^{-1} \left(K_1 - \omega_0^{i2} M_1 \right) U_0^i \tag{1}$$

It is built from a force residual $\left(K_1 - \omega_0^{i2} M_1 \right) U_0^i$, whose effect is measured by static displacement associated to this force, through the medium of flexibility matrix K_1^{-1}. This residual is homogeneous to a displacement, which is defined in each meshing point, and whose value is locally null if both structures are

identical. On the other hand, it can be either positive or negative, which means that one can not consider a minimizing approach of the problem, like shown in section 2.2.1. In order to get rid of this difficulty, one can take into account kinetic energy of this residual:

$$I^i = R^{iT} M_1 R^i \tag{2}$$

Then, one obtain a global value on the whole structure, which is always positive, and null if and only if $(K_1 - \omega_0^{i2} M_1)\, U_0^i = 0$. The problem is that this indicator is not local, that is why it can not be used as a localization tool. The local aspect is taken into account by considering the energy contribution I_e^i of each element to the total energy I^i:

$$I^i = \sum_e I_e^i \tag{3}$$

$$I_e^i = R^{iT} M_1^e R^i \tag{4}$$

In which M_1^e is the elementary mass matrix associated to element e. I_e^i is defined for each mode i on each element e of the structure, it is null if the finite element model equations are locally verified. This indicator will be used for the localization concerning mode i, but it can also be used to obtain a localization concerning a frequency range including n modes, in this case the mean indicator will be taken into account:

$$I_e = \frac{1}{n} \sum_{i=1}^{n} I_e^i \tag{5}$$

The local aspect considered here is related to the finite element model: the problem is supposed to be locally exact when nodal displacements and eigenfrequencies of structure Ω_1 lead to a null value if they are used in indicator 1, which does not mean that displacements and others fields are correct inside elements.

2.2 Relationships between chosen indicator and sensitivity of eigen characteristics

The purpose if this subsection is to link chosen indicator to eigen characteristics variations, it is valid for indicators 1 and 2: these are general results which can be applied in the particular field of finite element analysis.

2.2.1 Eigen frequencies variation

Eigen values are denoted $\lambda_0^i = \omega_0^{i2}$ and $\lambda_1^i = \omega_1^{i2}$. One suppose that characteristic operators of considered structures can be written in the following terms:

$$\begin{cases} K_1 = K_0 + \Delta K \\ M_1 = M_0 + \Delta M \end{cases} \tag{6}$$

Eigen characteristics are:

$$\begin{cases} U_1^i = U_0^i + \Delta U^i \\ \lambda_1^i = \lambda_0^i + \Delta\lambda^i \end{cases} \tag{7}$$

Modal equation i of structure 1 can be written:

$$K_1 U_1^i = \lambda_1^i M_1 U_1^i \tag{8}$$

After 6 and 7:

$$(K_0 + \Delta K)\left(U_0^i + \Delta U^i\right) = \left(\lambda_0^i + \Delta\lambda^i\right)(M_0 + \Delta M)\left(U_0^i + \Delta U^i\right) \tag{9}$$

Using modal equation of structure 0, pre-multiplying by U_0^{iT} and neglecting high order terms lead to the first-order equation:

$$U_0^{iT} K_0 \Delta U^i + U_0^{iT} \Delta K U_0^i = \Delta\lambda^i U_0^{iT} M_0 U_0^i + \lambda_0^i U_0^{iT} \Delta M U_0^i + \lambda_0^i U_0^{iT} M \Delta U^i \tag{10}$$

This can be simplified using modal equation of structure 1, $U_0^{iT} K_0 \Delta U^i = \lambda_0^i U_0^{iT} M \Delta U^i$, and assuming that eigen modes have been estimated using unit modal mass $U_0^{iT} M_0 U_0^i = 1$. The resulting equation is:

$$\Delta\lambda^i = U_0^{iT}\left(\Delta K - \lambda_0^i \Delta M\right) U_0^i \tag{11}$$

Which can also be written using equations 6:

$$\Delta\lambda^i = U_0^{iT}\left(K_1 - \lambda_0^i M_1\right) U_0^i \tag{12}$$

Finally, previous equation means that the residual force $(K_1 - \lambda_0^i M_1)\, U_0^i$, which has been used to build residual 1, and more precisely its work in the nominal displacement U_0^i, can be linked to frequency shifts between both structures. This analysis has been done using first order considerations; nevertheless, when differences are small, it allows one to link the proposed residual to the sensitivity of eigen frequencies, using only the solution of the nominal problem associated to a post-processing calculation.

One could think to use equation 12 in order to define a residual to localize, hoping to find contribution of each element to $\Delta\lambda^i$ shift, using elementary matrices in order to define an indicator such as $U_0^{iT}\,(K_1^e - \lambda_0^i M_1^e)\, U_0^i$. Unfortunately, this is not possible, since this indicator is globally null if both fields 1 and 0 are coincident, but this is not locally true: compensations between elements on which values are positive or negative induce a global null value. This is not the case with the proposed indicator, which is locally positive. However, equation 12 can be used to obtain informations about frequency shift induced by small structural modifications, with a very low calculation cost.

2.2.2 Link between residual estimation and eigen characteristics variations

Above calculation have shown that there is a close link between chosen indicator and eigen frequency shifts. However, the proposed relation is not explicit, where as it is possible to obtain complete expression of indicator 2 versus eigen modes and frequencies shifts, if one accept to develop eigen mode i of structure 0 on eigen basis of structure 1:

$$U_0^i = \sum_j \alpha_j^i U_1^j \tag{13}$$

This development is not always possible. In particular, if boundary conditions differ from one problem to another, the previous equation could be impossible to verify. Nevertheless, if differences between considered structures are reasonable, one can accept this development.

Eigenvalues shifts are again denoted $\Delta\lambda^i = \lambda_1^i - \lambda_0^i$. Residual 1 is:

$$R^i = U_0^i - \lambda_0^i K_1^{-1} M_1 U_0^i = U_0^i - \sum_j \alpha_j^i \frac{\lambda_0^i}{\lambda_1^j} U_1^j \tag{14}$$

Or:

$$R^i = \sum_j \alpha_j^i \left(1 - \frac{\lambda_0^i}{\lambda_1^j}\right) U_1^j \tag{15}$$

This allows one to develop expression of indicator 2:

$$I^i = R^{iT} M_1 R^i = \left(\sum_j \alpha_j^i \left(1 - \frac{\lambda_0^i}{\lambda_1^j}\right) U_1^j\right)^T M_1 \left(\sum_k \alpha_k^i \left(1 - \frac{\lambda_0^i}{\lambda_1^k}\right) U_1^k\right) \tag{16}$$

Which can be simplified using $U_1^{jT} M_1 U_1^k = \delta_{jk}$, in which δ_{jk} is Kronecker symbol:

$$I^i = \sum_j \left(\alpha_j^i \left(1 - \frac{\lambda_0^i}{\lambda_1^j}\right)\right)^2 \tag{17}$$

This leads to expression of indicator 2:

$$I^i = \left(\alpha_i^i\right)^2 \left(\frac{\Delta\lambda^i}{\lambda_1^i}\right)^2 + \sum_{j \neq i} \left(\alpha_j^i\right)^2 \left(1 - \frac{\lambda_0^i}{\lambda_1^j}\right)^2 \tag{18}$$

The first part of this equation has two factors: the first one, $\left(\alpha_i^i\right)^2$ is a term which is close to 1 if both vectors U_0^i and U_1^i are comparable, in other words if ΔU^i is small in equation 7. The second term is $\left(\frac{\Delta\lambda^i}{\lambda_1^i}\right)^2$, which is associated to the relative shift of squares frequencies of modes i. Then the first part of the indicator is closely connected to eigenfrequencies variations.

The second part of equation 18 shows influence of other modes than mode i: $\left(\alpha_j^i\right)^2$ is a measurement of the distance between eigen modes U_0^i and U_1^j with respect to U_1^j (it is the projection of U_0^i on U_1^j: its value is weak when ΔU^i is small), whereas the factor $\left(1 - \lambda_0^i/\lambda_1^j\right)^2$ is a weight whose value depends on the ratio λ_0^i/λ_1^j : for a given mode i, eigen value λ_0^i is fixed, and the factor has a large value if the decomposition needs modes U_1^j whose eigenvalues λ_1^j are lower than λ_0^i. The value of this factor is close to 1 if λ_1^j is greater than λ_0^i, like shown on figure 1: contribution of modes with higher eigenfrequencies is weaker than those with lower ones. This is in accordance with physical meaning: if low frequency modes are necessary for the modal decomposition, it means that

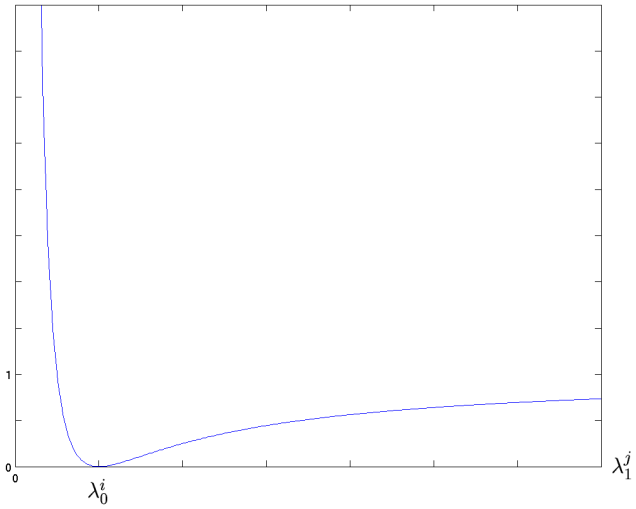

Fig. 1. Evolution of weight $\left(1 - \frac{\lambda_0^i}{\lambda_1^j}\right)^2$ versus λ_1^j.

significant differences exist between modes shapes, and this should have a large influence on indicator, while higher order modes correspond to representation of small differences, inducing smaller indicator values.

Finally, the first part of indicator 18 is a measurement of eigenfrequency shift, while the second one correspond to modes shapes variations.

2.3 Indicator choice conclusion

Choice of indicator 4 has been guided by those used in the field of finite element updating. It has been shown that with a few reasonable assumptions, it can be related to eigen characteristics variations, which allows one to justify its use to detect structural zones producing hypersensitive behavior. However, indicator choice is not sole, other expressions could have been used, but one will not detail this aspect here.

3 Finite element analysis of a plates network

3.1 Description of the considered structure

The first application of the proposed method in FE context is related to the structure on which this method has been first described analytically (6), (7). It

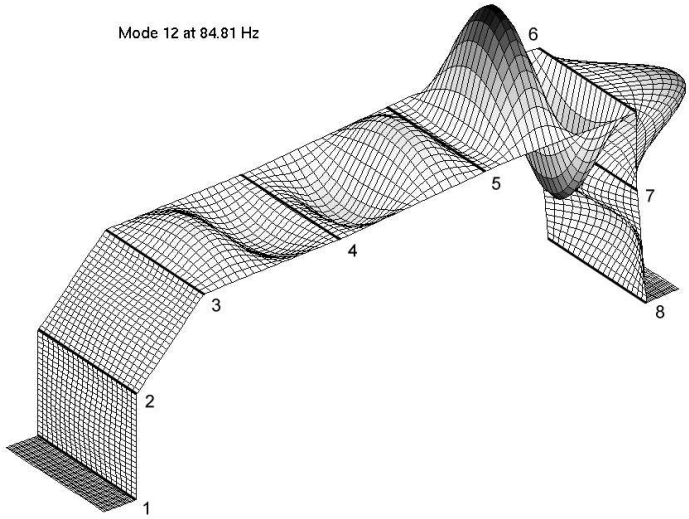

Fig. 2. Plates network: mode 12; coupling angles numbers.

is constituted by a network of plates which are simply supported on uncoupled edges. A finite element model of this structure has been developed, and 15 eigenfrequencies have been evaluated. One of these modes is represented on figure 2.

Variable parameters in this study are coupling angles, which are supposed to vary in a random way, according to a normal Gaussian repartition, centered on nominal angle value with a 1/6 degree standard deviation. In practice, corresponding angles belong to a one degree range. Using a Monte Carlo simulation, one can plot a sensitivity index for each eigenfrequency with respect to coupling angle. This index, which is the standard deviation of each eigenfrequency to mean of it ratio is plotted on figure 3. One can observe that coupling angles numbered 4, 5 and 7 are responsible for the main sensitivities, while other coupling angles are not sensitive. Physical meanings associated to this figure are detailed on appendix A.

3.2 Application of localization method

In order to apply the proposed method to the finite element model of the plates network, one should consider geometric modifications. Two ways can be used at this point. The first approach is a partial Monte Carlo simulation: a random choice of structural parameters belonging to manufacturing ranges is done in order to assembly mass and stiffness matrices, which are used with eigen data from the reference structure to perform calculation of indicator 4, and this is repeated as many times as necessary. The second strategy is to consider a single modified structure, built with parameters chosen at the edge of the

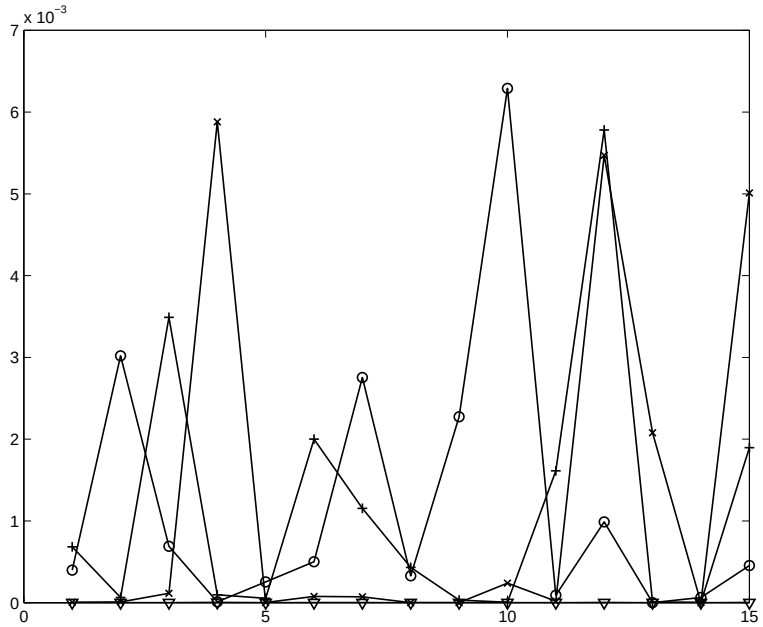

Fig. 3. Sensitivity of eigenfrequencies with respect to coupling angle, versus mode order. Monte-Carlo simulation, 50 calculations. -o-: Angle 4; -+-: Angle 5; -x-: Angle 7; -v-: Other angles.

range, in order to locally measure effects of variations. This is thinkable only if structural modifications are spatially independent, which is the case here. Therefore coupling angles of considered modified structure are nominal angles with a half degree shift. Then, assembly of matrices allows one to estimate the value of indicator 4, which is done for each mode. One can be interested by the most sensitive one, which is the tenth one, according to figure 3: consideration of figure 4 allows one to localize the zone which is responsible for dispersions. In this case, angle number 4 is well detected, and in particular the inner part of the plate, which is also the zone of large energy.

Similar results can be observed for modes 2 (fig. 5) , 4 (fig. 6) or 7 (fig. 7), on which angles responsible for largest sensitivities are well detected.

A particular case is the one of figure 8, which corresponds to mode 5, the zone in which the indicator has its largest value is located at the center of plate 2, although angle 4 zone is also detected. The indicator shows here some non local effects, however, according to figure 3, this mode is not hypersensitive to angle variation. The indicator is consistent to the fact as its maximum value is 1.2×10^{-6}, instead of 4×10^{-5} observed for mode 10.

As far as a global information on the frequency range is concerned, this fifth mode will be masked by other ones with higher sensitivities, like shown on figure 9, which represents the mean of indicator obtained considering 15 eigen modes. On this picture, one can observe that the 3 most sensitive coupling angles are well localized, while other ones do not appear on the structure.

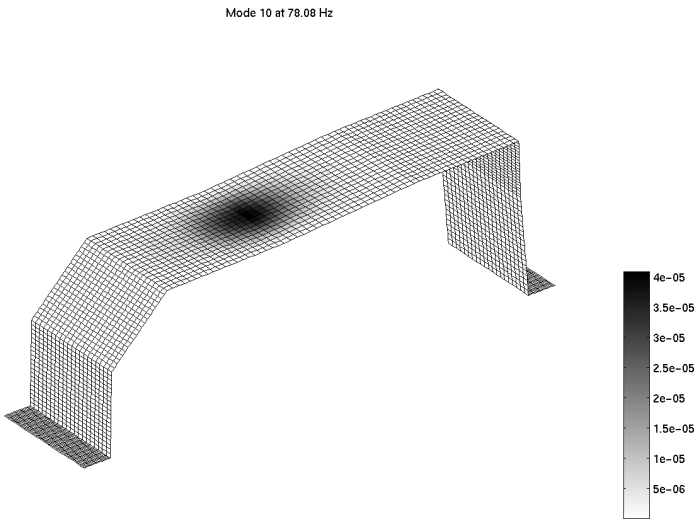

Fig. 4. Mode 10: indicator value.

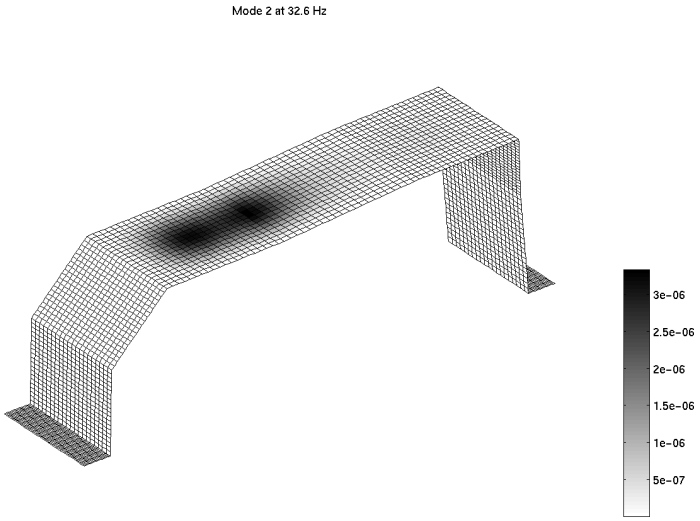

Fig. 5. Mode 2: indicator value.

More precise results can be obtained with an evaluation of indicator value for each coupling line: in the considered case, sensitivity of each line can be characterized with the sum of indicator values on each element located along the coupling line. Using this, one obtains figure 10, on which these values are plotted for each angle, versus mode number. This picture should be linked to sensitivity indicator (figure 3), and more precisely to figure 11, which have been obtained considering value $\left(\frac{\sigma(f_i^2)}{E(f_i^2)}\right)^2$, in which σ is the standard deviation and E is the mean of squared eigenfrequencies f_i^2, in order to be close to the term $\left(\frac{\Delta\lambda^i}{\lambda_1^i}\right)^2$ in equation 18. One should note that both plots can not be

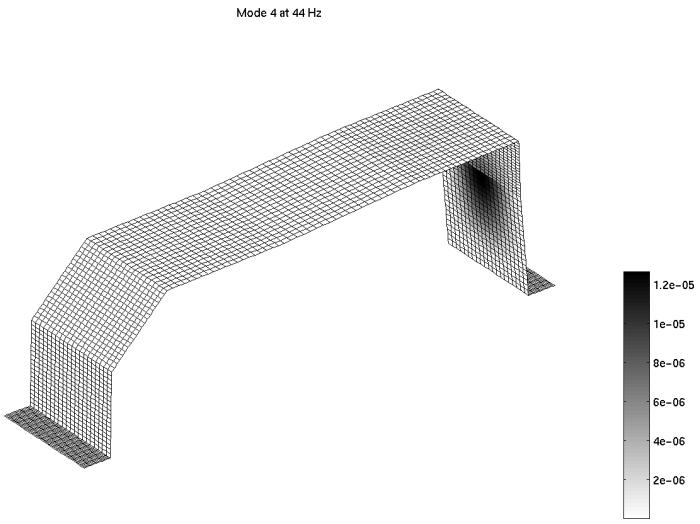

Fig. 6. Mode 4: indicator value.

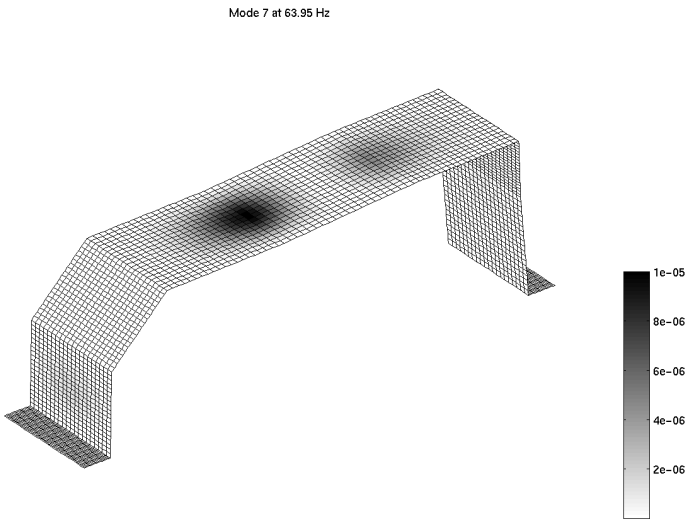

Fig. 7. Mode 7: indicator value.

identical, since they do not represent the same thing, in particular as far as the amplitude is concerned: in order to obtain a picture that would be close to figure 11, one should have considered independent variation of each coupling angle, which needs a higher calculation cost. However, one can observe that trends are comparable, and that the proposed indicator allows one to localize and to grade zones responsible for sensitive behavior with a low calculation cost.

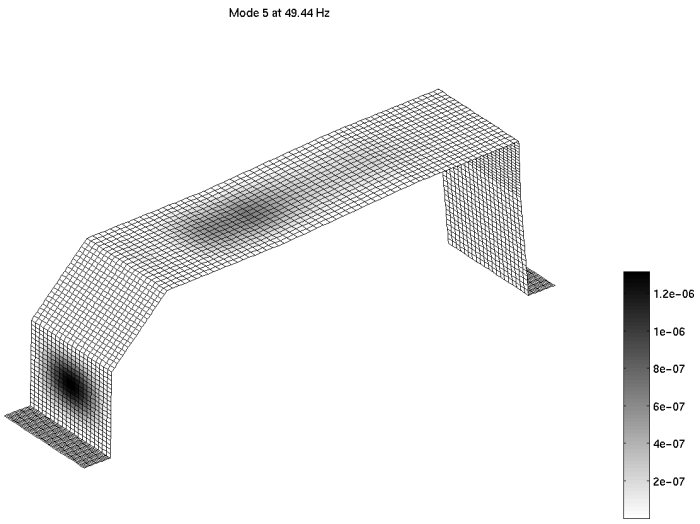

Fig. 8. Mode 5: indicator value.

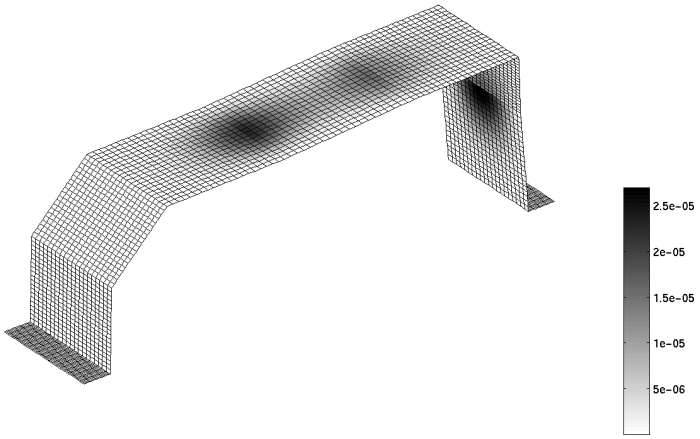

Fig. 9. Mean indicator, 15 eigen modes.

3.3 Conclusion

A method that allows one to detect structural zones responsible for hypersensitive behavior has been developed, and its implementation within a finite element code has been developed in order to test it on a FE model of a plates network, which is a well-known hypersensitive structure. Indicator choice has been detailed, and its expression has been linked to eigen data shifts. The plates network analysis has allowed one to find similar results to those obtained considering analytical application of the proposed method: localization of coupling lines responsible for sensitive behavior has been effective.

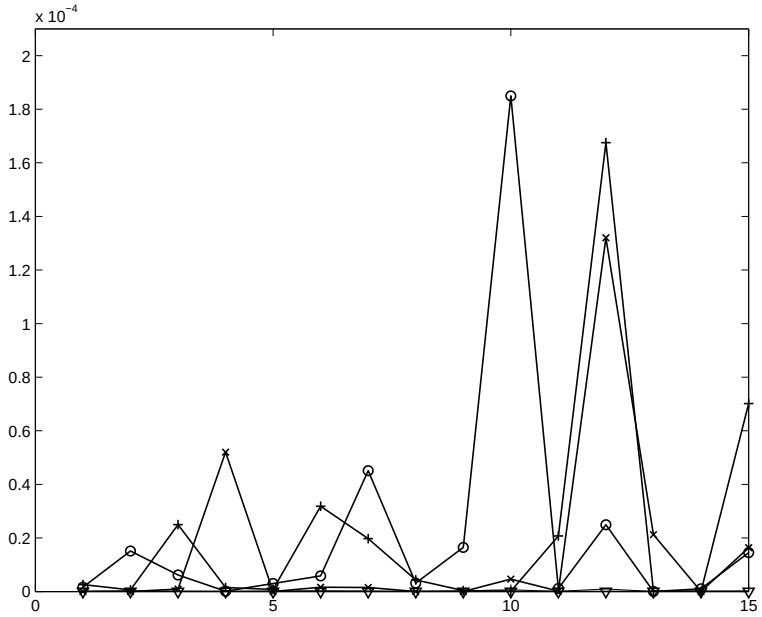

Fig. 10. Indicator value: sum on coupling lines adjacent elements, versus mode number. -o-: Angle 4; -+-: Angle 5; -x-: Angle 7; -v-: Other angles.

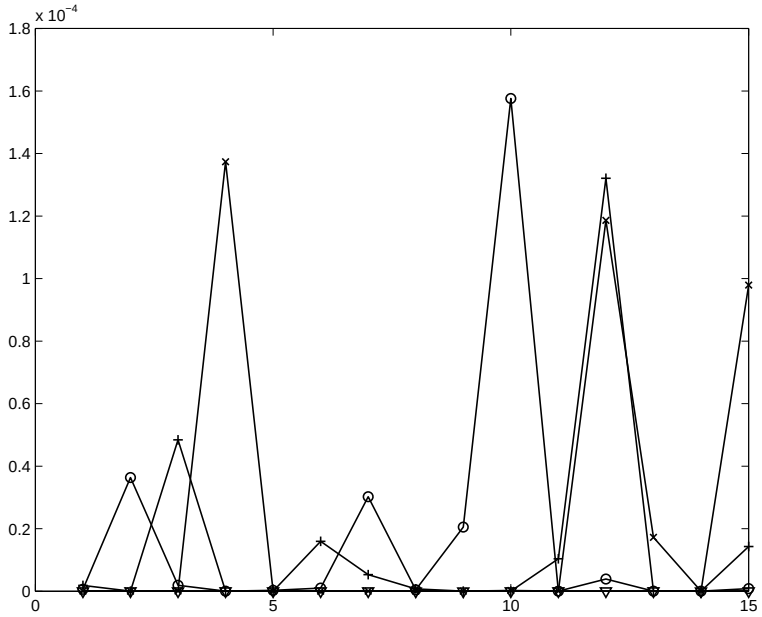

Fig. 11. Squared sensitivity of eigenvalues, with respect to coupling angle, versus mode number. Monte-Carlo simulation, 50 calculations. -o-: Angle 4; -+-: Angle 5; -x-: Angle 7; -v-: Other angles.

4 Finite element analysis of a cross member beam

4.1 Description and vibration behavior

4.1.1 Cross member beam description

Results presented above on an academic structure need to be completed with an industrial case. The proposed analysis is based on a cross member beam

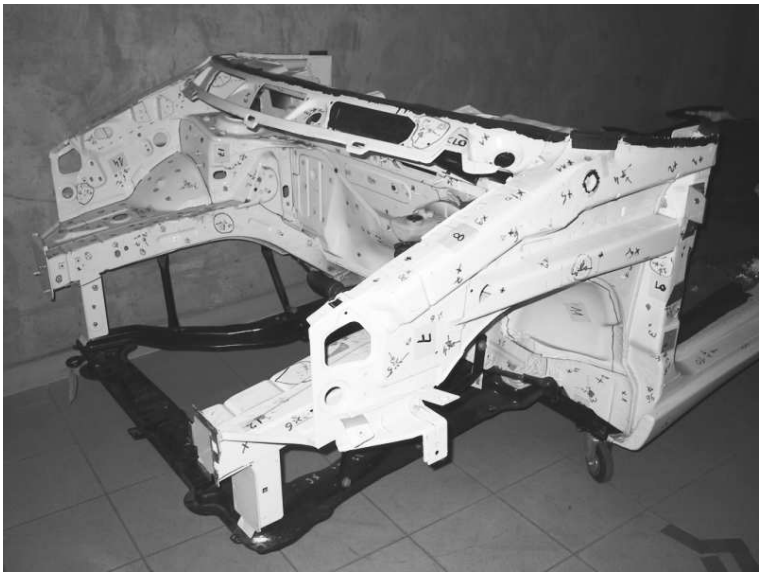

Fig. 12. Picture of cross member beam with some other constitutive parts of Peugeot 806 vehicle.

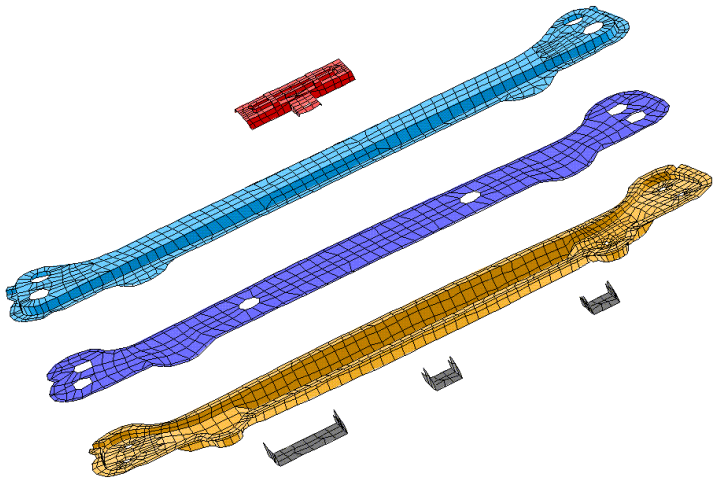

Fig. 13. 3D view of constitutive parts of the cross member beam.

of Peugeot 806 vehicle (picture 12), which is made up of three layers, joined by welding spots. These layers are presented on figure 13, as well as supports, which are also spot welded. The structure is supposed to be bolted along the four holes (2 on each side of the beam). The purpose of this analysis is to study sensitivity of welding spots positions, using the method described above. 82 plots are used to join the parts of the beam.

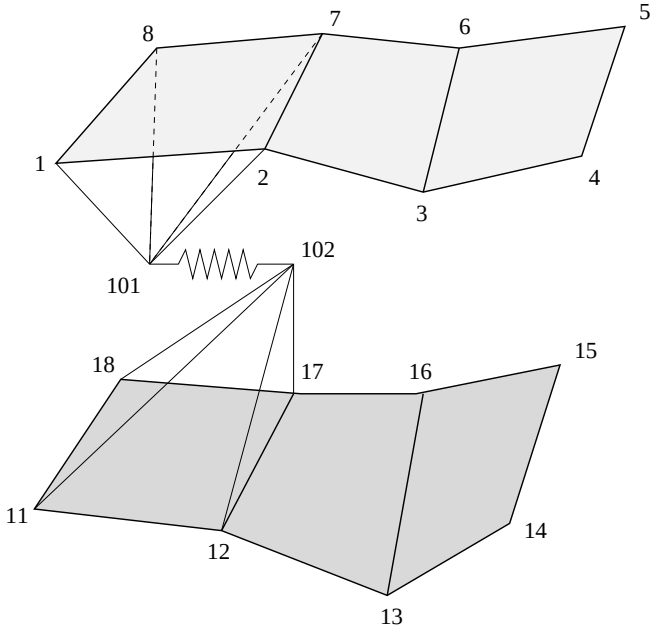

Fig. 14. Original mesh of a welding spot.

Mode	1	2	3	4	5	6	7	8	9	10
Eigen frequency (Hz)	110	240	302	380	521	568	591	599	653	673

Table 1
Original mesh eigen frequencies.

4.1.2 Numerical model of the beam

Cross member beam mesh has 17197 degrees of freedom, most of them are linked to nodes of CQUAD4 and CTRIA3 elements. As far as finite element model of welding spots used in this analysis is concerned, it is quite simple and presented on figure 14. The first part to be welded has nodes numbered 1 to 8, while the second one has nodes 11 to 18. Node 101 (resp. 102) does not belong to any of these parts and is used as a master node for a rigid RBE2 element with slaves nodes 1, 2, 7 and 8 (resp. 11, 12, 17, 18). Finally, six CELAS springs element are used to take into account rigidity of weld joint, linking nodes 101 and 102 along 6 degrees of freedom. This model is not the most accurate for description of behavior of welding spots, it is known to over estimate stiffness of joint, that is why more complex models using elements like RBE3 are generally used, nevertheless the proposed model is very simple to implement and results are convenient enough for the purpose of this analysis.

4.1.3 Vibrating behavior

Ten first eigenfrequencies of nominal structure are given in table 1. This is considered as the reference for the proposed analysis.

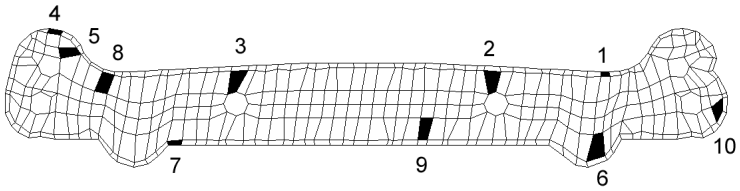

Fig. 15. Location of modified welding spots.

Mode	1	2	3	4	5	6	7	8	9	10
Eigen frequency (Hz)	109	221	235	296	369	412	480	519	549	564
Frequency shift (%)	1	8	22	22	29	28	19	13	16	16

Table 2
Eigen frequencies of reference model with 10 removed welding spots.

4.2 Analysis of influence of missing welding spots

During assembly process, some of the welding spots, which are done by robots, may be defective, or even missing. The purpose of this analysis is to find with a low calculation cost, which are the welding spots that should not be missing, at the risk of large eigen frequencies shifts.

4.2.1 Shifts due to missing welding spots

Among 82 welding spots, 10 have been arbitrarily chosen, they are linking intermediate layer to upper or lower one. These ten spots are described on figure 15.

The modified structure is then the reference one on which these 10 spots have been removed. As far as the numerical approach is concerned, this can be done by removing CELAS elements, or by canceling or imposing low values to associated stiffness coefficients. A numerical modal analysis on this modified structure allows one to verify that these ten welding spots have strong effects on vibrating behavior: in table 2, one can observe that frequencies shifts have large values, in particular as far as modes 5 and 6 are concerned, since corresponding shifts are worth up to 30%. These two modes are local ones, but frequencies shifts can be large also for global modes like numbers 3 and 4 which are both global flexural modes. Table 2 is illustrated on figure 16.

The purpose of the application of the proposed method is to find among ten removed welding spots which ones are responsible for observed frequencies shifts.

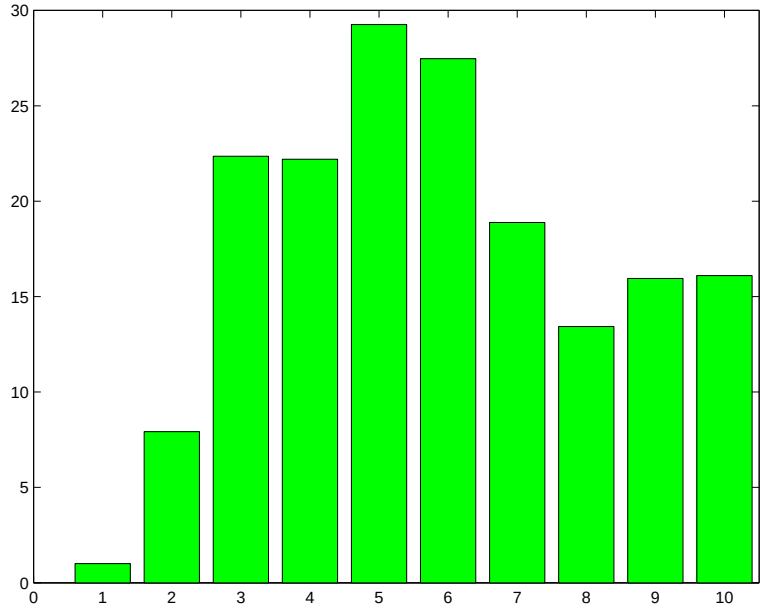

Fig. 16. Eigen frequencies shifts (%) versus mode number, original mesh with 10 removed welding spots.

4.2.2 Application of localization method

Thanks to local aspect of proposed residual, one can estimate effect of each welding spot using only one residual calculation, based on the reference structure with ten removed spots. This is thinkable while the analysis is limited to a few spots, since if a similar study would be done considering that all spots may miss, one should select only a set of them instead of the entirety of them, and several calculations would be necessary with judicious choice of missing welding spots. In the proposed analysis, this is not necessary since the number of modified welding spots is weak compared with the total number of spots, and moreover they are spatially independent, in other words for each element, there is at most one welding spot linked to it.

Equations presented on section 2.1 can not be applied directly on this problem because of rigid elements, inducing relationships between degrees of freedom of the model, which are responsible for impossibility of inversion of stiffness matrix K. This problem can be easily solved using projection matrix P of basis verifying rigid body connections. Matrices used in equations 1 and 4 are M_c and K_c:

$$M_c = P^T M P \ ; \ K_c = P^T K P \tag{19}$$

Matrix K_c is no longer rank deficient, and associated displacement fields are denoted U_c:

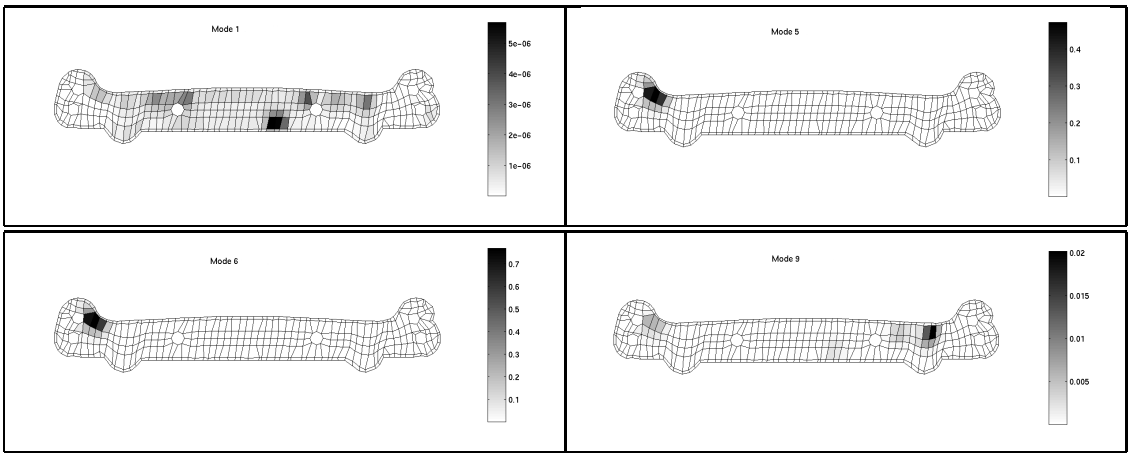

Fig. 17. Indicator repartition for modes 1, 5, 6 and 9.

$$U_c = P^T U \tag{20}$$

This operation induces reduction of degrees of freedom number, which is now 14824.

4.2.3 Results

Figure 17 shows indicator spatial repartition for modes 1, 5, 6 and 9. One can observe that both modes 5 and 6, which are the most sensitive ones, have similar location of element distribution large values. This zone corresponds to 3 welding spots, which are numbered 4, 5 and 8. As far as the first mode is considered, which has a very low sensitivity value according to figure 16, it induces weak element residual values.

A global information on the frequency range is obtained on figure 18, on which the mean value of element residual on frequency range corresponding to 10 eigen frequencies is drawn: the main differences which have been observed between reference structure and the one with missing welding spots are due to spots which are located near the upper left hole of the structure (spots 4, 5 and 8). Of course, second order differences are due to other welding spots, like the first one, which has been detected on mode 9 estimation (figure 17).

In order to verify that the localized welding spots are actually responsible for the main sensitivities, a numerical modal analysis can be performed on the reference structure with 3 missing welding spots which are the 3 ones located near the left hole (numbers 4, 5 and 8). Corresponding eigen frequencies are given in table 3.

These results have to be compared with table 2: this is done on figure 19, on

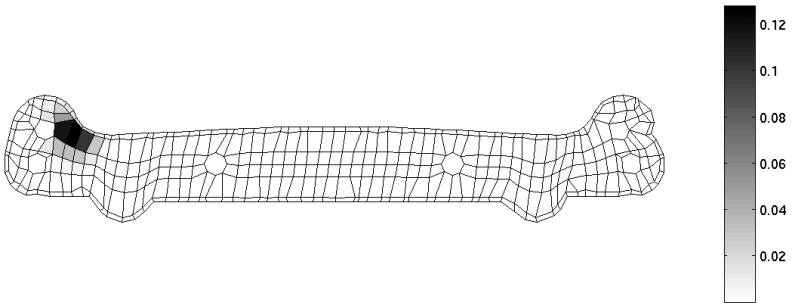

Fig. 18. Indicator mean value.

Mode	1	2	3	4	5	6	7	8	9	10
Eigen frequency (Hz)	109	222	237	299	373	412	530	590	597	652
Frequency shift (%)	0.4	8	22	21	28	27	10	2	9	3

Table 3
Eigen frequencies of reference model with three removed welding spots (numbers 4, 5 and 8).

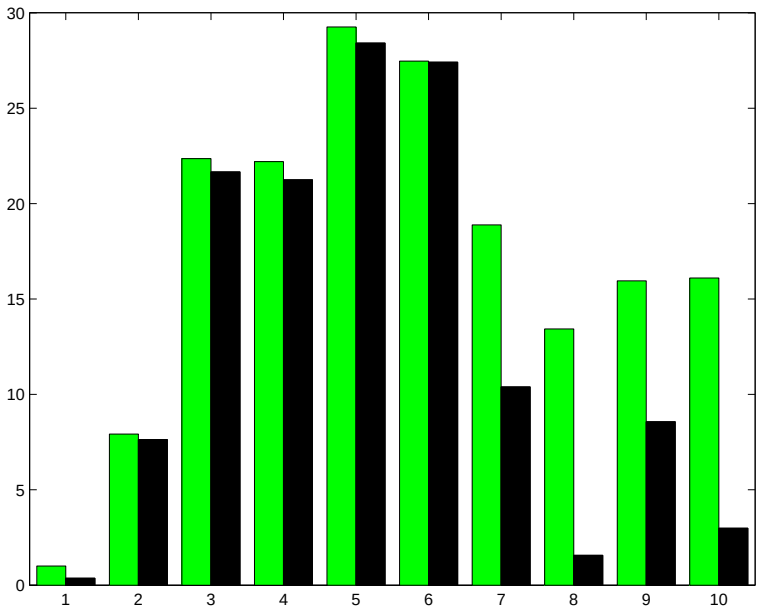

Fig. 19. Eigen frequencies shifts (%) versus mode number, original mesh with 10 removed welding spots (light bars) or 3 removed ones (numbers 4, 5, 8: dark bars).

which one can observe that the main differences between the reference structure and the one with 10 missing welding spots, corresponding to modes 3 to 6, are due to the three spots which have been detected by the indicator. Other differences, in particular those related to modes 7 to 10, which correspond to lower sensitivity values, are only partly due to these 3 welding spots.

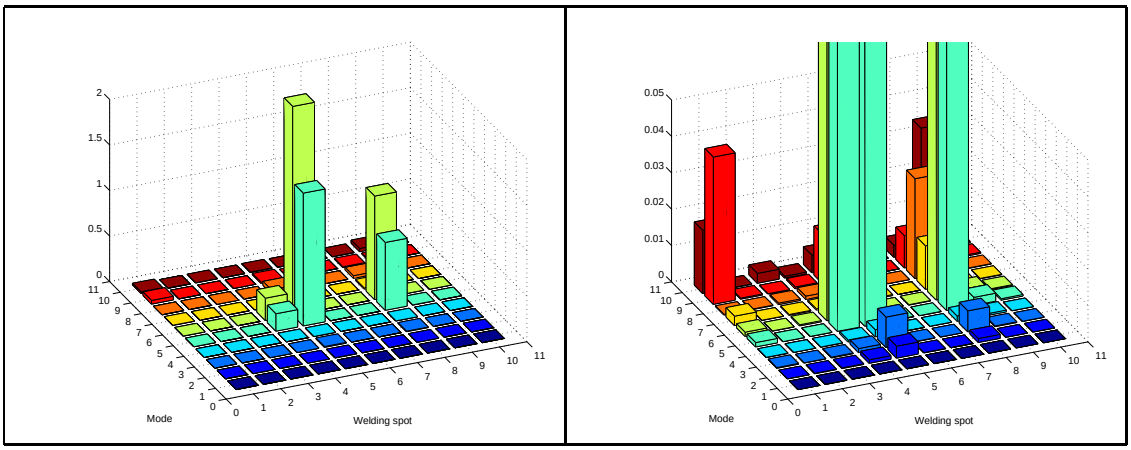

Fig. 20. Sensitivity indicator versus welding spot number and mode number.

Mode	1	2	3	4	5	6	7	8	9	10
Eigen frequency (Hz)	110	240	302	379	520	567	590	599	638	661
Frequency shift (%)	0.2	0.3	0.2	0.3	0.2	0.1	0.1	0.0	2.3	1.7

Table 4
Eigen frequencies of reference model with three removed welding spots (numbers 2, 6 and 7)

In order to confirm obtained results, a numerical modal analysis can be performed on the reference structure with 3 missing welding spots which have been detected as insensitive ones. For such an analysis, figure 18 is not precise enough, that is why one should use residual 4, and performing the sum of the indicator on adjacent elements to those described on figure 15. This allows one to obtain a residual value for each mode and each considered welding spot. Modes 5 and 6 have largest values on figure 20, which is of course in accordance with previous results, while the second part of the figure, which is a zoom of the first one, gives some informations about less sensitive spots, which are numbered 2, 6 and 7, or about sensitivities of modes 9 and 10, which are due to spots 1 and 9.

Results of modal analysis of the reference structure with missing spots 2, 6 and 7 are given in table 4.

These differences are compared with the ones obtained when 10 spots are missing on figure 21: one can observe that these three spots have very low effect on observed variations. One should note that this does not mean that these welding spots are useless, since there are other reasons (like static response) that vibration behavior on the considered frequency range for their existence.

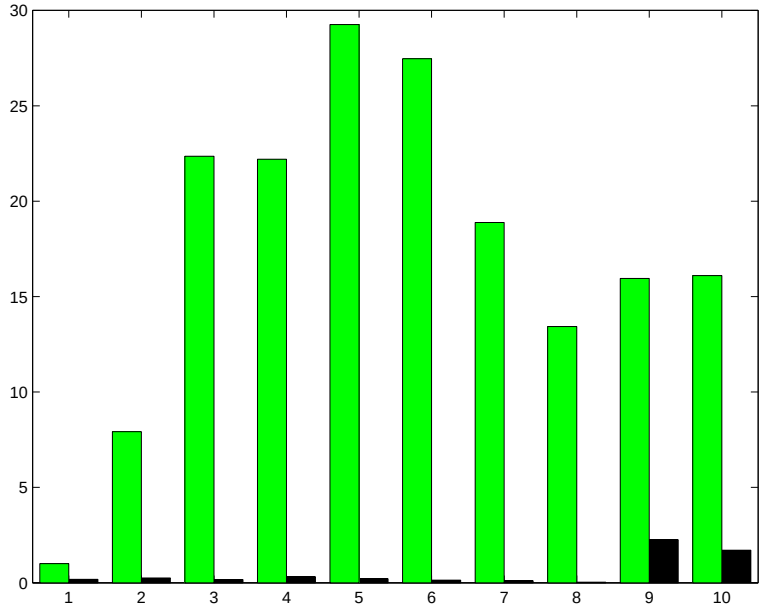

Fig. 21. Eigen frequencies shifts (%) versus mode number, original mesh with 10 removed welding spots (light bars) or 3 removed ones (numbers 2, 6, 7: dark bars).

4.2.4 Conclusion

With only one indicator evaluation done after resolution of nominal problem, most sensitive welding spots among the modified ones have been successfully detected, since a numerical modal analysis has been used to verify these results. Even if the number of considered welding spots is weak, it has been shown that the proposed method was able to detect and grade influence of each spot on a considered frequency range. As far as the location of the three detected welding spots is concerned, one can wonder why they are located on the left part of the cross member beam, since the structure seems to be symmetric. Two reasons can explain this fact: the first one is related to the shapes of the beam, which is not really symmetric, since one can observe differences between both end shapes and also on supports which are welded (figure 13). On the other hand, the main reason is that chosen ten welding spots are not symmetric, so spots which are "symmetric" to spots 4, 5 and 8 can not be detected. One can presume that a complete analysis considering that all welding spots could miss would induce an almost symmetrical repartition of influential welding spots.

5 Conclusion

Based on FEM updating techniques, a method that is able to detect structural zones which are responsible for hypersensitive behavior has been presented, and tested on both an academic case and an industrial structure. Compared to

classical approaches of the problem, this method requires a very low calculation cost, since the problem is solved only once, and then considering modified structures, an indicator is evaluated to localize zones on which differences can be observed. Expression of this indicator has been detailed, and linked to eigen characteristics variations. An academic plates network analysis has been presented, and coupling lines responsible for hypersensitive behavior have been successfully located on the structure. Application on an industrial cross member beam in order to study influence of welding spots positions has been developed, and results obtained using the method are very satisfactory and have been confirmed by a complementary finite element modal analysis.

A Appendix

On figure 3, one can associate sensitivities with modes shapes. As far as the frequency band of interest is concerned, in most of cases, angles corresponding to coupling of plates which are vibrating in phase opposition are less sensitive than coupling angles between in-phase vibrating plates. This can be observed on figure A.1, on which shapes of modes 1 and 2 are represented. For these two modes, the higher sensitivity correspond to mode 2, and is due to angle 4, which is the only coupling line with in-phase vibrating sides. Of course, sensitivities also exist for mode 1, even if mode shapes are phase opposed. This sensitivity can be explained using mode shape evolution: one can consider a simple structure made with two plates coupled with a null angle, in this situation the first mode is a bending mode with only one anti-node, since the structure is a single plate. When coupling angle grows up, it increases stiffness of the structure along coupling line, and the mode shape is constituted by two anti-nodes, which are vibrating in-phase, and also in phase with the weaker movement of the coupling line. So, the more the coupling angle grows up, the more the eigenfrequency grows up, while amplitude of displacement of coupling line grows down. As far as the mode 2 of the simplified structure is concerned (two plates coupled with a null angle), its mode shape has two anti-nodes which are vibrating out-of-phase around a nodal line that separates the structure in two identical parts. Increasing coupling angle will force the nodal line to coincide with the coupling line, inducing an eigen frequency increase, which is less important than the one induced by movement of coupling line canceling for mode 1. This is the phenomena that one can observe on figure A.1, except that the frequency shift of the initial first mode has induced it to be greater than the frequency of the mode with two anti-nodes. This modes shapes exchange is generally carried out without intersection of curves characterizing eigenfrequencies versus couple angle: modes shapes are varying in a continuous way from one shape to another, with no double eigenfrequency: this phenomena is known as curve veering (5), (4).

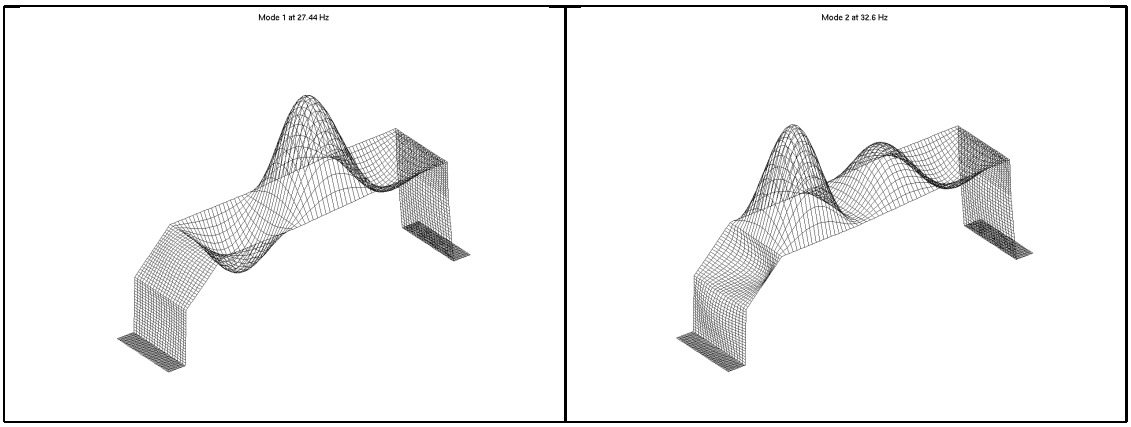

Fig. A.1. Plates network: modes 1 and 2.

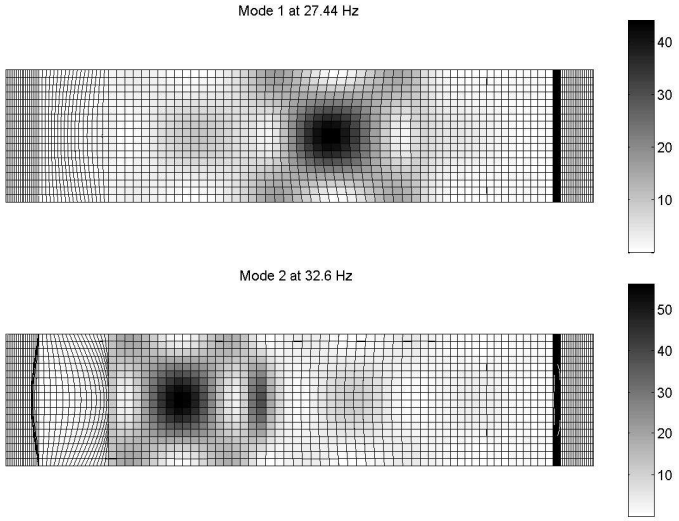

Fig. A.2. Plates network (upside view): potential energy repartition (modes 1 and 2).

Another way of understanding this higher sensibility of coupling angle 4 for mode 2 is to observe the potential energy repartition on the structure: as far as mode 2 is concerned, the potential energy along this coupling line has relatively large value, while for mode 1, its value is weaker. This means that a structural modification in the 4th coupling angle area will result in larger eigen data variations for mode 2 than for mode 1, although this energy criterion is not always sufficient to understand sensitivity phenomenon.

References

[1] M.I. Friswell and J.E. Mottershead 1995 *Finite Element Model Updating in Structural Dynamics*. Kluwer Academic Publishers.

[2] C.-P. Fritzen, D. Jennewein and T. Kieffer 1998 *Mechanical Systems*

and Signal Processing **12**, no. 1, 163–186. Damage detection based on model updating methods.

[3] R.G. Ghanem and R.M. Kruger 1996 *Computer Methods In Applied Mechanics And Engineering*, **129**, 289–303. Numerical solution of spectral stochastic finite element systems.

[4] J.R. Kutter and V.G. Sigillito 1981 *Journal of Sound and Vibration*, **75**, no. 4, 585–588. On curve veering.

[5] A.W. Leissa 1974 *Journal of Applied Mathematics and Physics*, **25**, no. 1, 99–111. On a curve veering aberration.

[6] M. Ouisse and J.L. Guyader 2003 *Journal of Sound and Vibration*, **260**, no. 1, 83–100. An energy residual method for detection of the causes of vibration hypersensitivity.

[7] E. Rebillard and J.L. Guyader 1997 *Journal of Sound and Vibration*, **205**, no. 3, 337–354. Vibrational behaviour of lattices of plates: basic behaviour and hypersensitivity phenomena.

[8] G.I. Schueller 2001 *Computers and Structures*, **79**, 2225–2234. Computational stochastics mechanics - recent advances.

[9] Z.Y. Shi, S.S. Law and L.M. Zhang 1998 *Journal of Sound and Vibration*, **218**, no. 5, 825–844. Structural damage localization from modal strain energy change.

[10] R. Bernhard 1996 *Proceedings of Inter-Noise 96, Liverpool, England*, 2867–2872. The limits of predictabiliy due to manufacturing and environmentally induced uncertainty.

[11] A. Bobillot and E. Balmès 2001 *IMAC 21, Kissimmee, Florida, USA*. Solving Minimum Dynamic Residual Expansion and Using Results for Error Localization.

[12] E. Blain, D. Aubry, P. Chove and P. Lardeur 1999 *Euromech 405: Numerical Modelling Of Uncertainties, Valenciennes, France*, 1–6. Influence of parameters dispersion on the vibrating behaviour of spot welded plates.

[13] H. Gysin 1990 *IMAC 8, Kissimmee, Florida, USA*. Comparison of expansion methods for FE modeling error localization.

[14] E. Balmes 2002. Structural Dynamics Toolbox For Use With Matlab, User's Guide Version 5. http://www.sdtools.com/